PLOS GENETICS

RESEARCH ARTICLE

CREB mediates the *C. elegans* dauer polyphenism through direct and cell-autonomous regulation of TGF-β expression

JiSoo Park[1], Hyekyoung Oh[2], Do-Young Kim[1], YongJin Cheon[1], Yeon-Ji Park[1], Hyeonjeong Hwang[1], Scott J. Neal[3], Abdul Rouf Dar[4], Rebecca A. Butcher[4], Piali Sengupta[5], Dae-Won Kim[2], Kyuhyung Kim[1,6]*

1 Department of Brain and Cognitive Sciences, DGIST, Daegu, Republic of Korea, **2** Department of Biochemistry, Yonsei University, Seoul, Republic of Korea, **3** Department of Neuroscience, SUNY Upstate Medical University, Syracuse, New York, United States of America, **4** Department of Chemistry, University of Florida, Gainesville, Florida, United States of America, **5** Department of Biology, Brandeis University, Waltham, Massachusetts, United States of America, **6** Korea Brain Research Institute (KBRI), Daegu, Republic of Korea

* khkim@dgist.ac.kr

Citation: Park J, Oh H, Kim D-Y, Cheon Y, Park Y-J, Hwang H, et al. (2021) CREB mediates the *C. elegans* dauer polyphenism through direct and cell-autonomous regulation of TGF-β expression. PLoS Genet 17(7): e1009678. https://doi.org/10.1371/journal.pgen.1009678

Editor: Coleen T. Murphy, Princeton, UNITED STATES

Received: September 30, 2020

Accepted: June 23, 2021

Published: July 14, 2021

Data Availability Statement: All relevant data are within the manuscript and its Supporting Information files.

Funding: This work was supported by the National Research Foundation of Korea (NRF-2020R1A4A1019436, NRF-2018R1A2A3074987) (K.K.) and (NRF-2017R1E1A1A01074980) (D.K.), and NIH R01GM087533 (R.A.B), and NSF IOS 1655118 (PS). The funders had no role in study design, data collection and analysis, decision to publish, or preparation of the manuscript.

Abstract

Animals can adapt to dynamic environmental conditions by modulating their developmental programs. Understanding the genetic architecture and molecular mechanisms underlying developmental plasticity in response to changing environments is an important and emerging area of research. Here, we show a novel role of cAMP response element binding protein (CREB)-encoding *crh-1* gene in developmental polyphenism of *C. elegans*. Under conditions that promote normal development in wild-type animals, *crh-1* mutants inappropriately form transient pre-dauer (L2d) larvae and express the L2d marker gene. L2d formation in *crh-1* mutants is specifically induced by the ascaroside pheromone ascr#5 (asc-ωC3; C3), and *crh-1* functions autonomously in the ascr#5-sensing ASI neurons to inhibit L2d formation. Moreover, we find that CRH-1 directly binds upstream of the *daf-7* TGF-β locus and promotes its expression in the ASI neurons. Taken together, these results provide new insight into how animals alter their developmental programs in response to environmental changes.

Author summary

C. elegans exhibits polyphenic development that is regulated by environmental conditions. Newly hatched larvae of *C. elegans* sense and integrate food availability and population density to determine whether to undergo normal reproductive development or arrest as non-aging, stress-resistant dauer. Dauer entry in *C. elegans* is proceeded by a commitment to either L2d, an obligate dauer precursor, or reproductive growth. Here, we find a *flp-8* neuropeptide gene as the bona fide L2d marker and show that the *crh-1* gene controls the L2d formation by direct regulation of *daf-7* TGF-β expression. Identification of this gene, as well as the novel L2d marker, now provides an unique opportunity to study the under-explored L2d formation of *C. elegans*.

Competing interests: The authors have declared that no competing interests exist.

Introduction

Animals exhibit phenotypic traits whose expression can be influenced by environmental signals, including temperature, food availability, and crowding. These signals are sensed, processed, and integrated by the nervous system, and govern appropriate developmental and/or behavioral phenotypes through effecting local and systemic changes in gene expression and/or endocrine signals. For example, population density and food supply determine wing development (winged vs. wingless) of the pea aphid (*A. pisum*) via ecdysone signaling [1]. This extreme form of phenotypic plasticity is referred to as polyphenism—the development of alternate and distinct phenotypes in animals of the same genotype—and is found across taxa [2,3]. Although the ability of animals to modulate their developmental programs in response to changing environmental conditions is crucial for their survival, the molecular mechanisms underlying such developmental plasticity are not yet fully understood.

The nematode *Caenorhabditis elegans* exhibits polyphenic development that is regulated by environmental conditions. Newly hatched L1/L2 larvae of *C. elegans* sense and integrate environmental signals, including food availability, temperature, and the abundance of pheromones (a population density indicator) to determine whether to undergo normal reproductive development into the L3 larval stage, or arrest at an alternate L3 stage, known as dauer. Dauer larvae are developmentally arrested, non-aging, stress-resistant, and can re-enter normal reproductive development if conditions improve [4,5] (Fig 1A). Under less favorable conditions, L1 larvae may transiently develop as L2d larvae, an obligate precursor to dauer commitment, but which still retain the capacity to resume reproductive development [4] (Fig 1A). Thus, worms assess and weigh multiple factors at multiple time points along the dauer trajectory in making the dauer decision. However, it is not clear how worms evaluate external and internal signals at specific developmental time windows and execute dauer formation. Specifically, the signals and molecules that promote the L1-to-L2d developmental transition are also not well understood.

C. elegans secretes pheromones, which are a complex cocktail of small molecules called ascarosides [6–9]. Moreover, worms produce and secrete distinct concentrations and combinations of ascarosides depending upon developmental stages and environmental conditions [7,10,11]. For example, ascarosides ascr#2 (asc-C6MK; C6), ascr#3 (asc-ΔC9; C9), and ascr#5 (asc-ωC3; C3), act as a dauer-inducing cue and worms produce specific concentrations of each ascaroside depending on cultivation conditions [6,7]. Although the potency and property of pheromone components in inducing dauer formation have been described, little is known about the contribution of each component to specific time windows along the dauer trajectory.

The molecular and genetic mechanisms underlying the decision to enter the dauer stage have been extensively studied, and have established two neuroendocrine *daf-7*/TGF-β and *daf-2*/insulin signaling pathways as critical mediators of this binary fate decision [12–14]. Expression of *daf-7* in the ASI sensory neuron type is regulated by environmental signals, including temperature, food availability, pheromone, and infection [12,13,15,16]. However, the mechanisms that regulate *daf-7* expression as a function of environmental conditions have not been fully described.

crh-1-encoded CREB (cAMP response element binding protein) plays critical roles in *C. elegans* metabolism, sensory responses, development, lifespan, and learning and memory [17–29] Similar to mammalian CREB, CRH-1 directly regulates target gene expression via the evolutionarily conserved cAMP-responsive element (CRE) and represents a nutritive or metabolic indicator [30]. However, a role for CREB in developmental plasticity, such as the decision to enter the dauer stage in *C. elegans*, has not been explored.

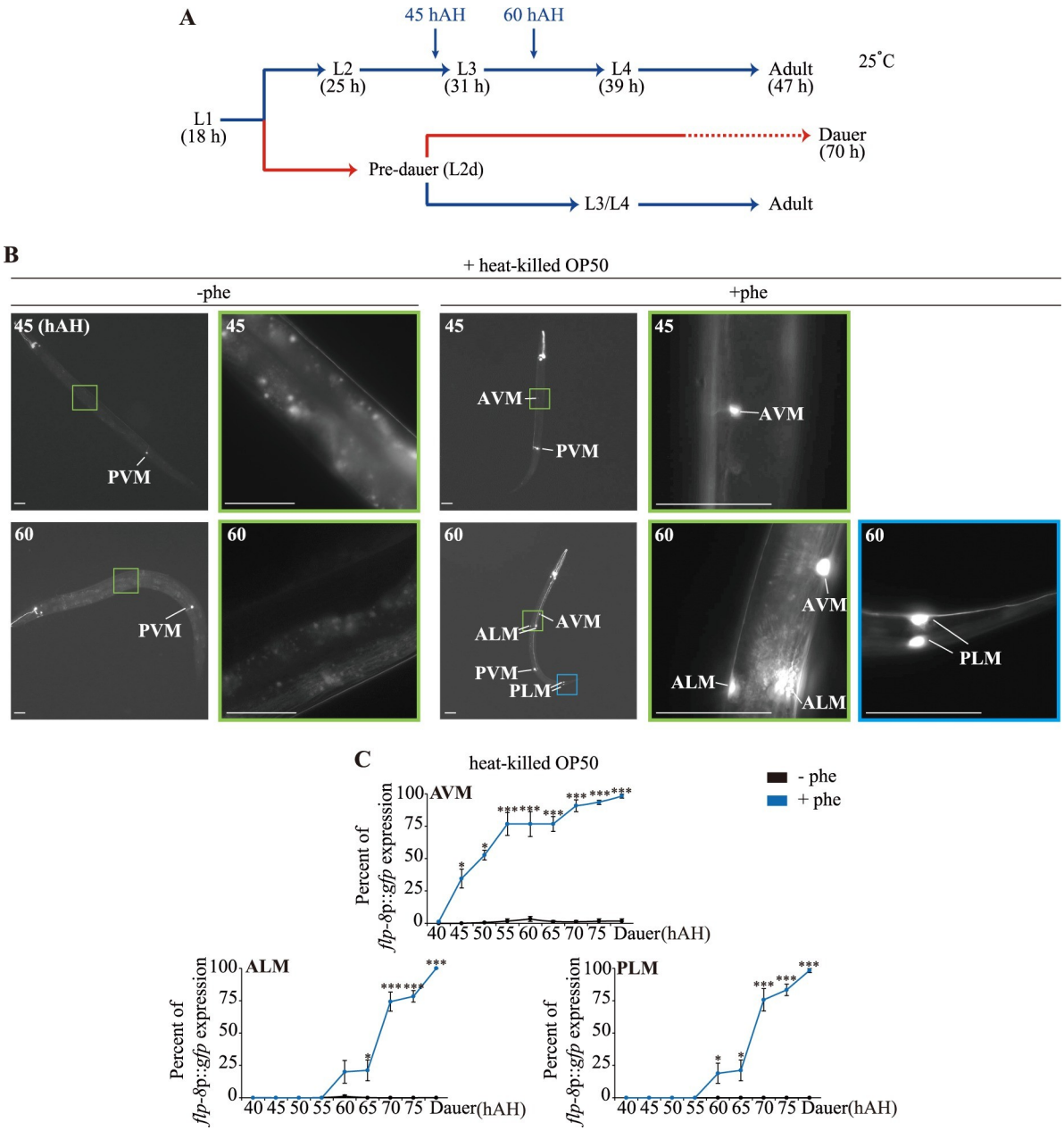

Fig 1. The *flp-8* expression is turned on in a subset of touch receptor neurons of L2d larvae. (A) *C. elegans* life cycle at 25˚C. In favorable conditions, newly hatched L1/L2 larvae undergo normal reproductive development into L3 larvae. Under unfavorable conditions, L1 larvae arrest as dauer larvae via the L2d pre-dauer stage. Under less favorable conditions, L1 larvae transiently become L2d larvae, which can resume reproductive growth. Numbers show the approximate duration in hours of development of each stage or hours after hatching (hAH). **(B)** Representative images of wild-type animals expressing *flp-8*p::*gfp* in a subset of touch receptor neurons in the presence of heat-killed OP50 food without (left column) or with (right three columns) ascr#5 pheromone. The color-matched boxed regions of the second column are shown at higher magnification. hAH, hour after hatching. Scale bars: 50 μm. **(C)** Percent of *flp-8*p::*gfp* expression in the AVM, ALM, and PLM neurons by wild-type animals when grown in the presence of heat-killed OP50 food and the presence or absence of ascr#5 pheromone. n ≥ 30 for each. Error bars indicate SEM. * and *** indicate different from wild-type at $p < 0.05$ and $p < 0.001$, respectively (student t-test).

https://doi.org/10.1371/journal.pgen.1009678.g001

Here, we show that CRH-1 plays a role in the decision to enter the L2d stage. In rich food conditions, pheromone is generally insufficient to induce L2d/dauer formation in wild-type animals. However, *crh-1* mutants exhibit transient L2d formation and express the L2d marker

gene *flp-8* under such conditions. L2d formation of *crh-1* mutants is induced by ascr#5, but not by ascr#2 or ascr#3, and expression of CRH-1 in the ascr#5-sensing ASI neurons is sufficient to rescue inappropriate L2d formation in *crh-1* mutants. We find that CRH-1 acts cell-autonomously in the ASI sensory neurons to regulate *daf-7* TGF-β expression and that ASI-specific overexpression of *daf-7* is sufficient to block L2d formation in *crh-1* mutants. We also identify a functional CRE in *daf-7* regulatory sequences and show that it is specifically bound by CRH-1, confirming that CRH-1 regulates *daf-7* expression in ASI. Together, these results reveal that CREB modulates developmental plasticity by repressing L2d entry in the presence of rich food sources and abundant ascr#5, via direct regulation of *daf-7* TGF-β expression in the ascr#5-sensing ASI neurons.

Results

A *flp-8* FMRFamide-like neuropeptide gene is expressed in a subset of touch receptor neurons in pre-dauer larvae

To better understand the mechanisms underlying L2d larvae formation, we first screened for a marker that specifically identifies the L2d developmental stage. The *flp-8* FMRFamide-like gene was previously shown to be differentially expressed in a subset of touch receptor neurons (AVM, ALM, PLM; referred to as AAP-TRN henceforth) in dauer larvae in addition to expression in the AUA, URX and PVM neurons throughout larval development [31]. We monitored the onset and maintenance of *flp-8*p::*gfp* reporter gene expression in the AAP-TRN of animals grown under non-dauer-inducing conditions and dauer-inducing conditions with limited heat-killed OP50 food and with and without the ascr#5 pheromone, respectively [32]. Consistent with the previous study [31], we detected the expression of *flp-8*p::*gfp* in AVM only in the dauer-inducing conditions (Fig 1B and 1C). Compared to non-dauer-inducing conditions, expression in AVM was first detected 40 h after hatching (hAH) with more prominent expression evident at 60 hAH; 60 hAH is approximately 20 h prior to dauer entry/commitment under these conditions (Fig 1B and 1C). Animals expressing *flp-8*p::*gfp* in the AVM neurons at 60 hAH were morphologically similar to dauer larvae but did not survive under 1% sodium dodecyl sulfate (SDS) [5] treatment (S1 Fig), implying that *flp-8* expression in the AVM neurons begins at the L2d stage, before the completion of dauer cuticular remodeling that confers resistance to this detergent. We noted the onset of *flp-8* expression in the ALM and PLM neurons at 55 hAH, five hour prior to dauer entry (Fig 1B and 1C). All dauer larvae expressed *flp-8*p::*gfp* in the AAP-TRN (Fig 1B and 1C). Moreover, *flp-8*p::*gfp* was expressed in the AAP-TRN of *daf-7* mutant larvae (S2 Fig). Taken together, these results suggest that the onset of *flp-8*p::*gfp* expression in the AVM neurons and possibly the ALM and PLM neurons can be used as a marker for the L2d stage.

crh-1 CREB mutants express L2d marker genes in non-dauer-inducing conditions

In a specific non-dauer-inducing condition with abundant live OP50 food and high concentrations of ascr#5, we found that about 25% *crh-1* mutant larvae inappropriately expressed the *flp-8* reporter gene in the AAP-TRN, which is significantly different from wild-type larvae (Fig 2A and 2B). However, in dauer-inducing conditions with limited heat-killed OP50 food and high concentrations of ascr#5 pheromone, the expression of *flp-8* in *crh-1* mutant larvae in AAP-TRN was similar to that of wild-type, although a slightly smaller percentage of *crh-1* mutants expressed GFP in the AAP-TRN as compared to wild-type (S3 Fig). All assays were conducted in this non-dauer inducing condition with abundant live OP50 food unless noted

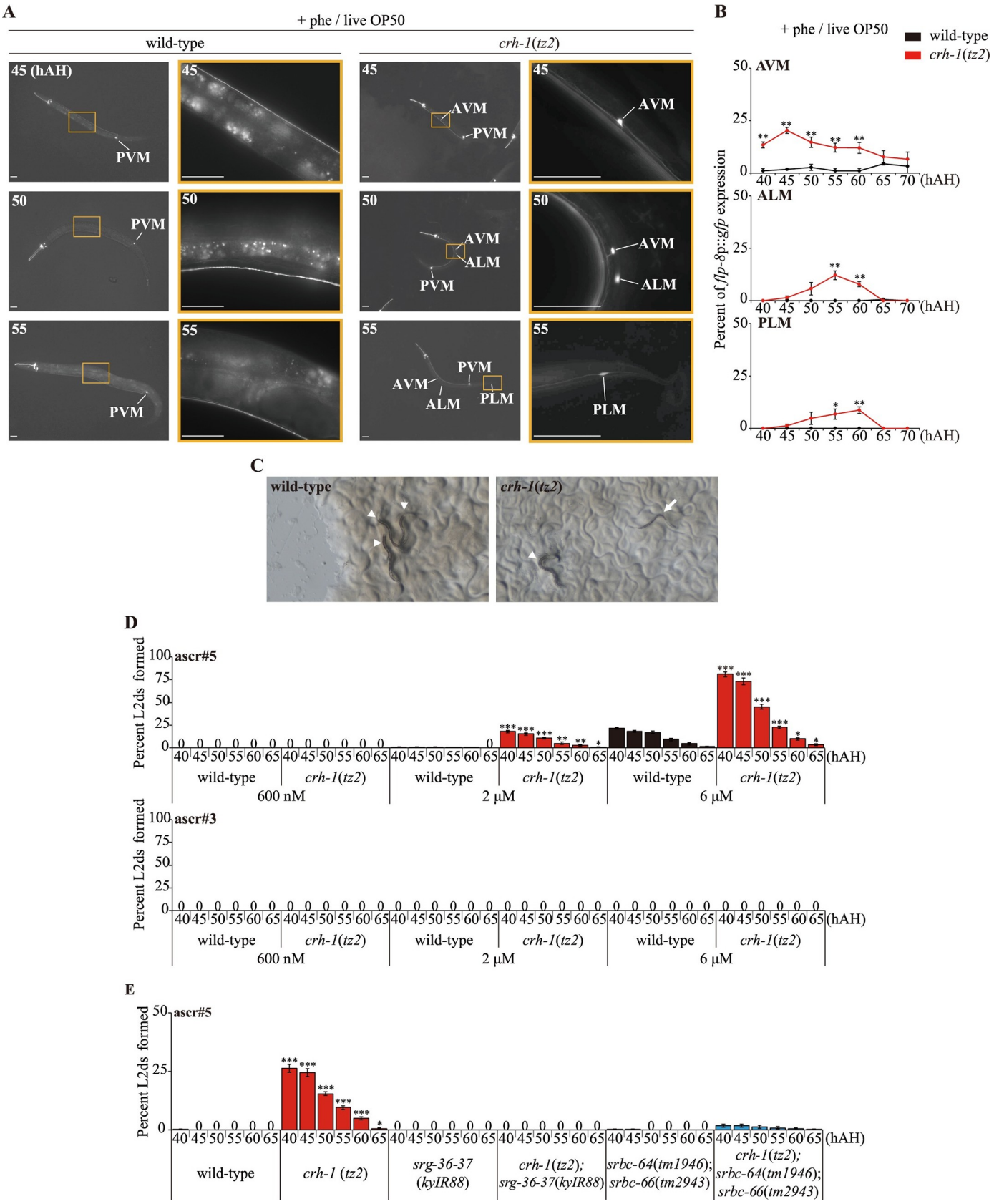
A
+ phe / live OP50
wild-type
crh-1(tz2)
45 (hAH)
PVM
AVM
ALM
PLM
50
55
B
+ phe / live OP50
wild-type
crh-1(tz2)
AVM
ALM
PLM
Percent of flp-8p::gfp expression
(hAH)
C
wild-type
crh-1(tz2)
D
ascr#5
ascr#3
Percent L2ds formed
wild-type
crh-1(tz2)
600 nM
2 µM
6 µM
E
ascr#5
Percent L2ds formed
wild-type
crh-1 (tz2)
srg-36-37 (kyIR88)
crh-1(tz2); srg-36-37(kyIR88)
srbc-64(tm1946); srbc-66(tm2943)
crh-1(tz2); srbc-64(tm1946); srbc-66(tm2943)

Fig 2. *crh-1* mutants inappropriately express an *flp-8* L2d marker gene and form transient pre-dauer L2d larvae in non-dauer inducing conditions. (A) Representative images of wild-type (left column) or *crh-1* mutant (right two columns) animals expressing of *flp-8*p::*gfp* in a subset of touch receptor neurons in the presence of live OP50 food and ascr#5 pheromone. The color-matched boxed regions of the second column are shown at higher magnification. hAH, hour after hatching. Scale bars: 50 μm. **(B)** Percent of *flp-8*p::*gfp* expression in the AVM, ALM and PLM neurons by wild-type or *crh-1* mutant animals when grown in the presence of live OP50 food and ascr#5 pheromone. n ≥ 30 each. **(C)** Light microscopy images of wild-type (left) or *crh-1* mutant (right) animals in the presence of live OP50 and crude pheromone. Arrowhead or arrow indicates a L3 or L2d larva, respectively. **(D)** Percent of L2d formed by wild-type or *crh-1* mutant animals when grown in the presence of live OP50 food and ascr#5 (top) or ascr#3 (bottom) pheromone. N ≥ 5 for each. **(E)** Percent of L2d formed by animals of the indicated genotypes when grown in the presence of live OP50 food and ascr#5 pheromone. N ≥ 8 for each. Error bars indicate SEM. *, **, and *** indicate different from wild-type at $p < 0.05$, $p < 0.01$, and $p < 0.001$, respectively (student t-test **(B, D)** or one-way ANOVA with Bonferroni's post hoc tests **(E)**).

https://doi.org/10.1371/journal.pgen.1009678.g002

otherwise. The onset of expression in these neurons in *crh-1* mutants under non dauer-inducing conditions was approximately 35 hAH, five hours earlier than in the dauer-inducing condition, likely due to their rapid growth from having live food available [33]. *flp-8* expression was not observed in the AAP-TRN of wild-type or *crh-1* mutant larvae in the absence of pheromone (S4 Fig), indicating that the exposure to pheromone is necessary for induction of *flp-8* expression in the AAP-TRN. An additional genetic marker, *nhr-246* transcription factor, for the L2d stage was also expressed in the intestine of *crh-1* mutant larvae [34] (S5 Fig). These results show that *crh-1* mutants inappropriately express L2d marker genes in conditions that do not promote dauer formation in wild-type animals.

crh-1 mutants inappropriately form transient pre-dauer L2d larvae upon exposure to ascr#5

To better understand the *crh-1* mutant phenotype, we next examined the ability of *crh-1* mutants to enter the dauer stage in response to different concentrations of ascaroside pheromones, under standardized dauer-inducing conditions. We found that *crh-1* mutants exhibited normal or weakly decreased pheromone-mediated dauer formation (S3 Fig). However, in a non-dauer inducing condition with abundant live OP50 food and high concentrations of crude pheromone, *crh-1* mutants formed thin dauer-like larvae 40–60 hAH (Figs 2C and S4) consistent with inappropriate induction of the L2d stage. To assess whether these larvae were indeed dauers, we treated them with 1% SDS. None of the *crh-1* dauer-like larvae survived under 1% SDS treatment (S1 Fig), indicating that these larvae have not fully remodeled their cuticle as expected for dauer larvae. We next characterized their morphology using scanning electron microscopy. The mouths of *crh-1* dauer-like larvae remained open as in L3 larvae (S6 Fig), suggesting, in combination with their other phenotypic attributes, that they are indeed L2d larvae. Moreover, by 65 hAH, these larvae had resumed reproductive development, consistent with transient passage through the L2d state and incongruent with dauer commitment and exit.

To determine whether the transient L2d formation of *crh-1* mutants is induced by specific pheromone components, we tested several ascaroside pheromones, including ascr#2, ascr#3, and ascr#5. All assays were conducted beginning 40 hAH unless noted otherwise. We found that *crh-1* mutants specifically formed transient L2d in the presence of micromolar concentrations of ascr#5, but not ascr#2 or ascr#3 (Figs 2D and S7). Moreover, *flp-8* was not expressed in the AAP-TRN of *crh-1* mutant larvae in response to ascr#2 and ascr#3 (S8 Fig).

ascr#5-mediated dauer formation has been shown to be primarily mediated by a pair of GTP-binding protein (G protein)-coupled receptors (GPCRs), SRG-36 and SRG-37 expressed specifically in ASI, and partly by another pair of GPCRs, SRBC-64 and SRBC-66 expressed in the ASK sensory neurons [15,35]. We found that the transient L2d formation of *crh-1* mutants was suppressed completely by mutations in both *srg-36* and *srg-37* and partially by mutations in both *srbc-64* and *srbc-66* (Fig 2E), supporting the specificity of ascr#5 in the transient L2d formation of *crh-1* mutants. Taken together, these results imply that *crh-1* mutants

inappropriately and transiently enter into the L2d stage in response to ascr#5 prior to resuming reproductive development.

crh-1 acts in the ASI neurons to regulate ascr#5-mediated L2d formation

To identify the molecular mechanisms by which CRH-1 regulates ascr#5-mediated L2d formation, we identified the site of action of CRH-1. Previously, *crh-1* had been shown to be expressed in a set of head neurons of adult *C. elegans* [17,24]. To further verify the expression patterns of *crh-1*, we generated transgenic animals expressing GFP under the control of sequences 2601 bp, 2411 bp, 1094 bp, or 737 bp (*crh-1*p*1*::*gfp* to *crh-1*p*4*::*gfp*) upstream of the translation start sequence of *crh-1* gene. We found that 2601, 2411, and 1094 bp regulatory sequences drove limited-expression possibly due to lack of certain *cis*-regulatory sequences [21,23] and showed expression specifically in three pairs of sensory neurons in the head amphid organs, including in the AWC, ASE, and AFD neurons, consistent with previous observations [24]. However, we also routinely detected weak GFP expression in the ASI sensory neurons (Fig 3A and 3B). Strong GFP expression of the *crh-1*p*4*::*gfp* transgene was detected exclusively in the ASI neurons throughout larval development (Fig 3A and 3B). Expression of wild-type *crh-1* cDNA sequences driven by *crh-1*p*1* or *crh-1*p*4* promoters were both partially sufficient to suppress L2d formation of *crh-1* mutants (Fig 3C), suggesting that *crh-1* acts in the ASI sensory neurons. The morphology and dye-filling properties of the ASI neurons were not altered by the *crh-1* mutation ($n > 50$ each) (S9 Fig), suggesting that CRH-1 does not play a general role in ASI neuron development.

To confirm these findings, we next rescued *crh-1* mutant phenotypes by expressing *crh-1* cDNA under the control of cell-specific promoters, including *srg-47* (ASI), *ceh-36*Δ (AWC), and *ttx-1* (AFD) [17]. Whereas expression of *crh-1* in single AWC or AFD neurons did not rescue the L2d formation defects of *crh-1* mutants, ASI-specific expression rescued the phenotype to the same extent as expression driven under the endogenous *crh-1* promoter (Fig 3D). ASI-specific expression of *crh-1* also fully rescued the *flp-8* expression defects of *crh-1* mutants (Fig 3E). Taken together, we conclude that the *crh-1* gene is expressed in and functions in the ASI neurons to regulate L2d formation.

daf-7 TGF-β expression is decreased in the ASI neurons of *crh-1* mutants

Identification of the ASI neurons as the site of action for CRH-1 prompted us to investigate whether CRH-1 also plays a role in regulating the expression of the *daf-7* transforming growth factor-β (TGF-β), which is expressed mainly in ASI, and which plays a major role in dauer formation [12,13]. A feasible hypothesis for the inappropriate entry of *crh-1* mutants into the L2d stage is that the expression of *daf-7* is downregulated in *crh-1* mutants under non-dauer-inducing conditions. Previously, the *daf-7* expression has been monitored using either an integrated *daf-7*p::*gfp* reporter gene, or by single-molecule fluorescence *in situ* hybridization (smFISH) [16,36]. We found that the *daf-7*p::*gfp* reporter exhibited decreased expression in the ASI neurons of *crh-1* mutants (Fig 4A and 4B). The ASI-specific expression of *crh-1* restored *daf-7*p::*gfp* expression in *crh-1* mutants (Fig 4B). We next used smFISH to accurately examine the endogenous transcriptional activity of *daf-7* and observed that the fluorescence intensity of *daf-7* FISH probes in the ASI neurons was also decreased in *crh-1* (Fig 4A and 4C). Moreover, ascr#5 further decreased *daf-7* transcriptional activity (Fig 4C). These results demonstrate that CRH-1 is necessary to maintain a robust expression of *daf-7* in the ASI neurons.

Similar to *daf-7* expression, the expression of a candidate *str-3* chemoreceptor gene in the ASI neurons is regulated by exposure to pheromones [15,36]. Expression of an *str-3*p::*gfp* reporter gene was strongly decreased in *crh-1* mutants. This gene expression phenotype was

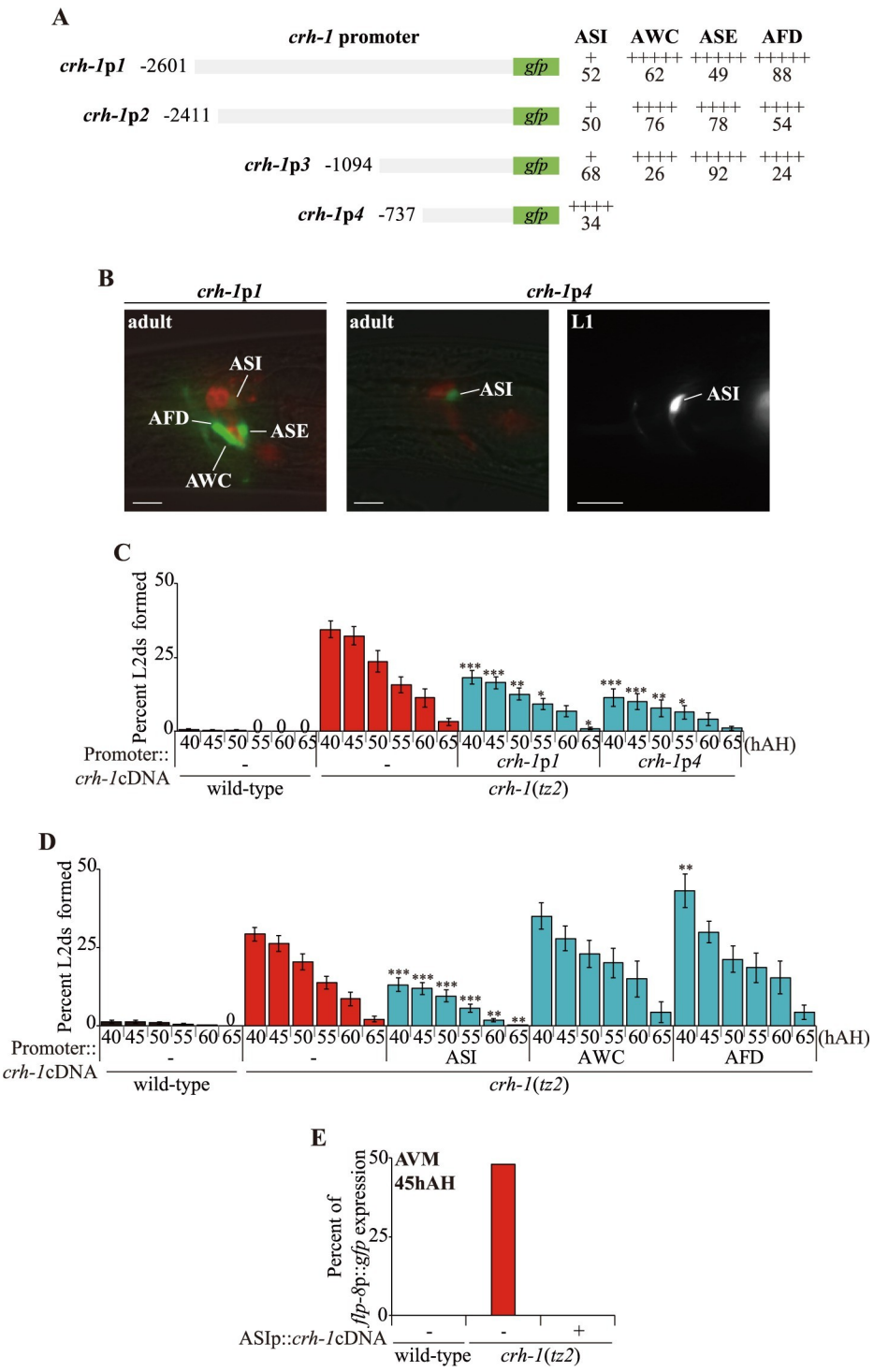

Fig 3. *crh-1* is expressed and acts in the ASI neurons to regulate ascr#5-mediated L2d formation. (A) The percentage of adult transgenic animals expressing *crh-1p1*:: *gfp*, *crh-1p2*::*gfp*, *crh-1p3*::*gfp* or *crh-1p4*::*gfp* reporter construct in the indicated neurons is shown. The strength of GFP expression is indicated by the number of + symbols. At least two independent extrachromosomal lines for each construct were examined. n ≥ 60 for each. **(B)** Representative images of adult or L1 larval transgenic animals expressing *gfp* expression under the control of *crh-1* promoter*1* (*crh-1p1*) and *crh-1* promoter*4* (*crh-1p4*). Adult animals were dye-filled with DiI. Scale bar: 10 μm. **(C and D)** Percent of L2d formed by animals of the indicated genotypes when grown in the presence of live OP50 food and ascr#5 pheromone. N ≥ 6 for each. Error bars indicate SEM. *, **, and *** indicate different from *crh-1* mutants at

$p < 0.05$, $p < 0.01$, and $p < 0.001$, respectively (one-way ANOVA with Bonferroni's post hoc tests). **(E)** Percent of *flp-8*p::*gfp* expression in the AVM neurons by animals of the indicated genotypes when grown in the presence of live OP50 food and ascr#5 pheromone. $n \geq 45$ for each.

https://doi.org/10.1371/journal.pgen.1009678.g003

again rescued by ASI-specific expression of *crh-1* (Fig 4D and 4E). Taken together, these results are consistent with the hypothesis that CRH-1 mediates transcriptional regulation of *daf-7* TGF-β and *str-3* GPCR gene expression in the ASI neurons.

daf-7 TGF-β signaling is required for the ascr#5-mediated L2d formation of *crh-1* mutants

daf-7 null mutants form dauers constitutively (Daf-c) regardless of environmental conditions, although other conditions and mutants in which *daf-7* expression is perturbed result in less penetrant dauer-related phenotypes [12]. We, therefore, investigated whether reduced *daf-7* expression plays a role in the inappropriate induction of L2d larvae in *crh-1* mutants. As expected, 100% of *daf-7* mutants formed L2d with abundant live OP50 food and high concentrations of ascr#5 (Fig 5A). Compared to the transient L2d formation of *crh-1* mutants, *daf-7* L2d larvae committed to dauer entry. In addition, *flp-8* expression in the AVM neurons of *daf-7* mutants initiated at 40 hAH and lasted throughout the L2d and dauer stages (Fig 5B and 5C). To confirm that DAF-7 acts downstream to CRH-1 in regulating dauer formation, we overexpressed DAF-7 specifically in the ASI neurons of *crh-1* mutants and found that it partially suppressed the L2d formation of *crh-1* mutants (Fig 5D). Moreover, DAF-7 expression in the ASI neurons partially rescued the L2d formation phenotype of *daf-7* mutants (Fig 5E), further supporting a role of the ASI neurons in the L2d formation of *crh-1* mutants.

It was previously shown that the Daf-c phenotype of *daf-7* mutants was suppressed by loss-of-function mutations of the *daf-3* SMAD or *daf-5* SNO/SKI transcription factor genes [37,38], whereas mutation of *daf-16* represses Daf-c mutations in the insulin signaling pathway [14]. We found that the loss of *daf-5* function fully suppressed the L2d phenotype of *crh-1* mutants, whereas the loss of *daf-3* or *daf-16* function did not affect the L2d formation of *crh-1* mutants (Figs 5F and S10). These results suggest that *daf-5* acts downstream of *crh-1* in ascr#5-mediated L2d formation and that the *daf-7* TGF-β signaling pathway mediates the L2d formation of *crh-1* mutants.

CRH-1 directly regulates *daf-7* expression via a conserved CRE motif

Like mammalian CREB, CRH-1 can act as a sequence-specific transcription factor to regulate gene expression via cAMP-response elements (CRE; TGACGTCA) [39] (Fig 6A). To determine whether CRH-1 directly regulates the expression of *daf-7* in the ASI neurons, we first analyzed the promoter regions of the *daf-7* gene. Although we could not identify any DNA sequences which showed exact matches to the CRE site within 3.1 kb upstream of the *daf-7* initiator codon, we identified ten DNA sequences that contain the consensus ACGT CRE core sequence within this sequence (Fig 6B). We mutated these sequences in the context of the *daf-7*p::*gfp* reporter gene, and found that mutations in one specific sequence, "GTACGTAC" located ~2380 bp upstream of the translational start site caused decreased *daf-7*p::*gfp* expression in the ASI neurons (Fig 6B and 6C). This mutation did not affect the faint reporter expression we observed in ASJ neurons (S11 Fig), indicating the specificity of this motif in the regulation of ASI expression of *daf-7* [16]. Moreover, the decreased ASI *daf-7* expression by mutations of the CRE site was not altered in *crh-1* mutant adults (Fig 6D). These results support our hypothesis that CRH-1 binds this putative CRE in the *daf-7* promoter to regulate its expression in ASI neurons.

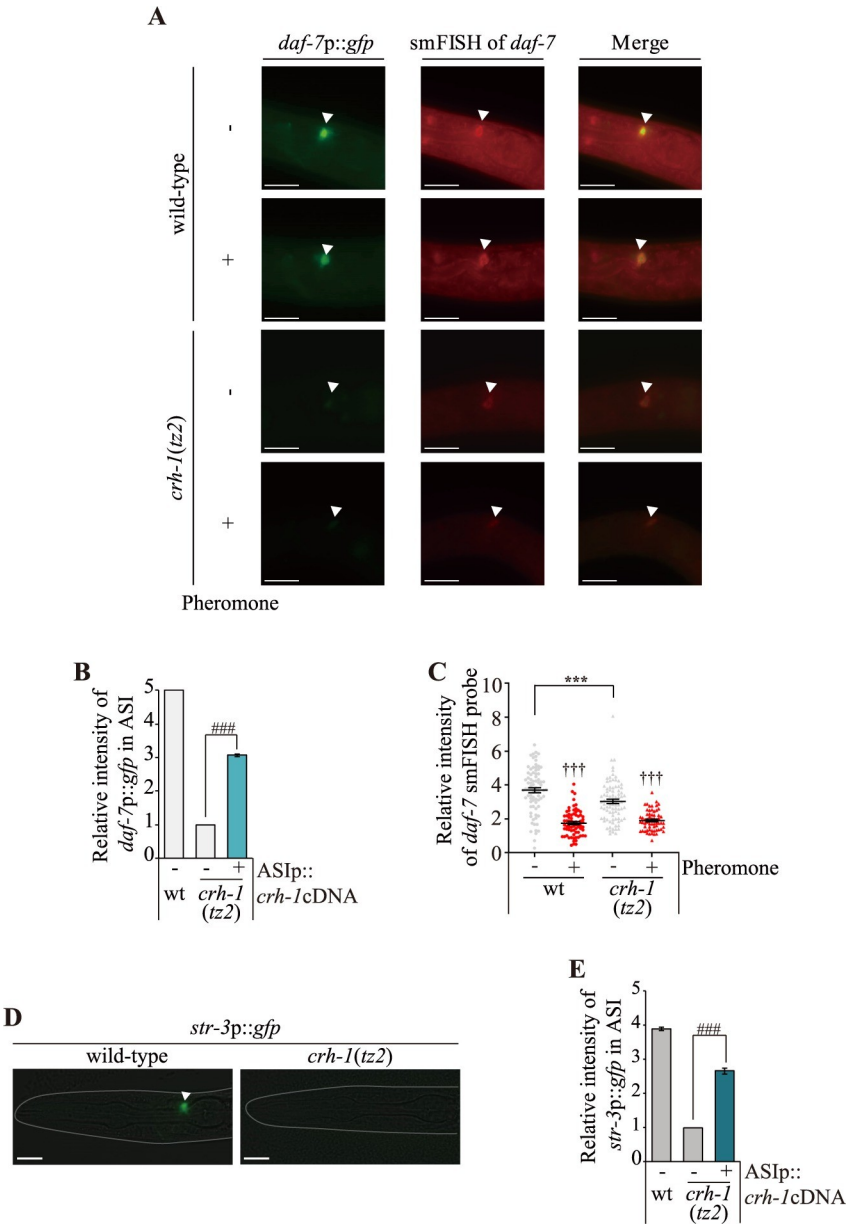

Fig 4. *crh-1* mutants exhibit a decrease of *daf-7* expression in the ASI neurons. (A) Representative images of L1 larval wild-type or *crh-1* mutant animals expressing *daf-7*p::*gfp* transgene in the presence (+) or absence (-) of ascr#5. Shown is GFP expression or *daf-7* smFISH signal in the ASI neurons. All images for wild-type versus *crh-1* mutant animals were taken with identical camera settings, including the same exposure time. Anterior is to the left. Scale bar: 50 μm. **(B)** The relative level of *daf-7*p::*gfp* fluorescence in the ASI neurons of L1 larval animals of the indicated genotypes in the absence (-) of ascr#5. **(C)** Scatter plot of fluorescence intensity of *daf-7* smFISH signal in the ASI neurons of wild-type or *crh-1* mutant animals in the presence (+) or absence (-) of ascr#5. The median is indicated by a horizontal line. Each dot is the fluorescence intensity of a single neuron; n ≥ 30 neurons total each, at least two independent experiments. **(D)** Representative images of L1 larval wild-type or *crh-1* mutant animals expressing *str-3*p::*gfp* in the ASI neurons. Scale bar: 10 μm. **(E)** The relative level of *str-3*p::*gfp* fluorescence in the ASI neurons of L1 larval animals of the indicated genotypes in the absence (-) of ascr#5. n ≥ 30 for each. Error bars indicate SEM. ***, †††, or $^{\#\#\#}$ indicates different from wild-type, absence of ascr#5, or *crh-1* mutants at $p < 0.001$, respectively (student t-test). Arrowheads indicate the ASI neurons **(A and D)**.

https://doi.org/10.1371/journal.pgen.1009678.g004

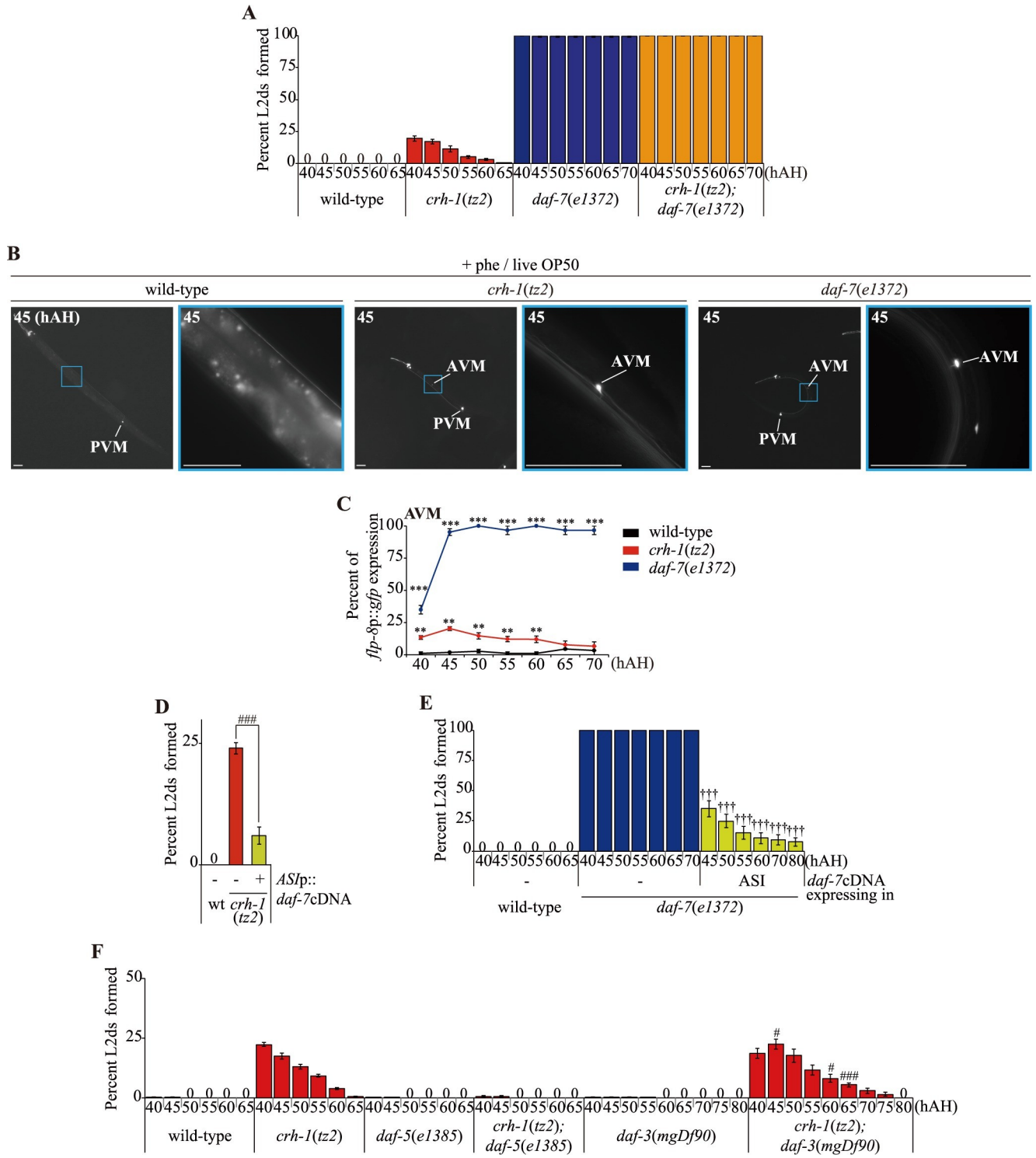

Fig 5. *daf-7* mediates the ascr#5-mediated L2d formation of *crh-1* mutants. (A) Percent of L2d formed by animals of the indicated genotypes when grown in the presence of live OP50 food and ascr#5 pheromone. N ≥ 4 for each. **(B)** Representative images of wild-type (left column), *crh-1* mutant (middle columns), or *daf-7* mutant animals expressing of *flp-8*p::*gfp* in a subset of touch receptor neurons in the presence of live OP50 food and ascr#5 pheromone. The color-matched boxed regions of the second column each are shown at higher magnification. hAH, hour after hatching. Scale bars: 50 μm. Images of wild-type and *crh-1* mutants are originated from Fig 2B. **(C)** Percent of *flp-8*p::*gfp* expression in the AVM neurons by animals of the indicated genotypes when grown in the presence of live OP50 food and ascr#5 pheromone. n ≥ 30 for each. *** indicates different from wild-type at $p < 0.001$(student t-test). **(C-E)** Percent of L2d formed by animals of the indicated genotypes when grown in the presence of live OP50 food and ascr#5 pheromone. N ≥ 8 **(C)**, 6 **(D)**, 4 **(E)** for each. Error bars represent the SEM. ### or ††† indicates different from *crh-1* or *daf-7* mutants at $p < 0.001$, respectively (student t-test).

https://doi.org/10.1371/journal.pgen.1009678.g005

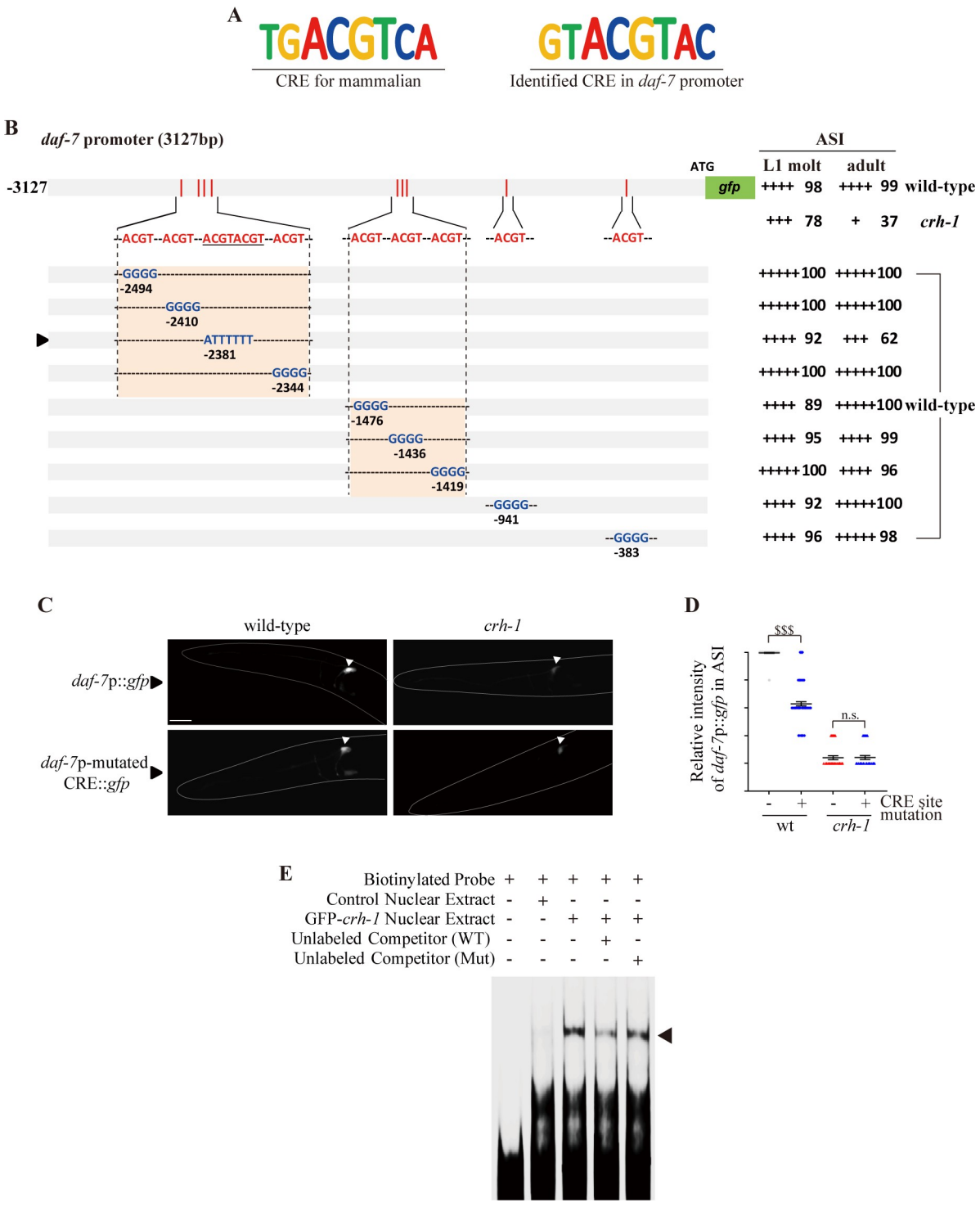

Fig 6. CRH-1 directly binds a CRE motif in the *daf-7* promoter. (A) Shown are the conserved mammalian CRE motif and the newly identified CRE motif in the *daf-7* promoter. **(B)** The percentage of transgenic animals expressing *daf-7*p:: *gfp* reporter construct in the ASI neurons is shown. GFP fluorescence was observed either in wild-type or *crh-1* mutant animals. The strength of GFP expression is indicated by the number of + symbols. Wild-type nucleotides are indicated in red, mutated nucleotides in blue. An arrowhead indicates *daf-7*p-mutated CRE promoter. At least two independent extrachromosomal lines for each construct were examined. n ≥ 30 for each. **(C)** Representative images of L1 larval wild-type or *crh-1* mutant animals expressing *daf-7*p::*gfp* or *daf-7*p-mutated CRE::*gfp* in the ASI neurons. Scale bar: 50 μm. **(D)** Scatter plot of fluorescence intensity of *daf-7*p::*gfp* fluorescence in the ASI neurons of adult wild-type or *crh-1* mutant animals with (+) or without (-) of CRE site mutation. The median is indicated by a horizontal line. Each dot is the fluorescence intensity of a

single neuron; n ≥ 30 neurons total each, at least two independent experiments. Error bars represent the SEM. $^{\$\$\$}$ indicates different at $p < 0.001$, respectively (student t-test). **(E)** Nuclear extracts isolated from control (2nd lane) or GFP-*crh-1* (3rd, 4th, 5th lane) transfected cells were analyzed by EMSA using biotinylated *daf-7*p-CRE probes (2nd, 3rd, 4th, 5th lane) with non-biotinylated *daf-7*p-WT-CRE (4th lane) and *daf-7*p-Mut-CRE (5th lane) competitors as indicated. An arrowhead indicates a complex of CRE probes and CRH-1.

https://doi.org/10.1371/journal.pgen.1009678.g006

To confirm the direct binding of CRH-1 to this CRE motif *in vitro*, we performed electrophoretic mobility shift assays (EMSA) on cultured HEK293T cells. Specific CRE binding activity was evident in GFP-CRH-1 overexpressing nuclei, and absent in control nuclear extract (Fig 6E). Furthermore, this CRE binding activity was significantly diminished by co-incubation with wild-type non-biotinylated probes, whereas mutant unlabeled probes failed to effectively compete (Fig 6E). While these results need to be further confirmed *in vivo*, they indicate that CRH-1 can directly bind to the CRE motif identified in the *daf-7* promoter sequence, which, in turn, may enhance *daf-7* expression in the ASI neurons.

Thus, we have identified CRH-1 as a critical mediator of ASI state in developing *C. elegans*. CRH-1 promotes the expression of *daf-7* in the presence of pheromone and abundant food to suppress inappropriate passage through L2d, which ultimately delays reproductive maturation of the animal and may be disadvantageous to fitness.

Discussion

Dauer entry in *C. elegans* is gated by sequential developmental decisions, first, at L1 to transition to either L2 or L2d, and second, a commitment to either diapause or reproductive growth (Fig 1A). Precociously or inadvertently entering dauer has the potential to carry a large fitness cost for an animal, given the rapid development and fecundity of *C. elegans*. Here we have shown that the CREB homolog CRH-1 is a key regulator of the first decision, whether or not to enter L2d. *crh-1* mutants inappropriately express the L2d marker gene *flp-8* in ALM, AVM, and PLM neurons and transiently form L2d larvae in non-dauer-inducing conditions. However, *crh-1* mutants do not commit to dauer entry in the absence of additional environmental cues and thus ultimately make the correct developmental decision. Our data support a model in which CRH-1 positively regulates dauer-inhibiting *daf-7* TGF-β expression in the ascr#5-sensing ASI neurons (Fig 7). The loss of *crh-1* function leads to decreased *daf-7* TGF-β expression, which provides a sensitized genetic background for further ascr#5-mediated *daf-7* TGF-β repression via SRG-36/37 GPCRs (Fig 7). When the *daf-7* expression is eliminated, animals constitutively enter the dauer state, and thus *daf-7* expression serves as a critical rheostat for the determination of *C. elegans* developmental trajectory [12,13,15]. Our results demonstrate that worms exploit distinct strategy and molecules at different dauer decision points and CRH-1 acts in ASI and gates the initial L1-to-L2d decision in response to pro-growth environmental signals (food), prior to dauer commitment, and thus *crh-1* mutant provides a unique opportunity to study the under-explored L1 to L2/L2d transition. Previously, Lakhina and coworkers showed that *crh-1* mutants develop more slowly than wild-type animals at 20˚C in the presence of food due to a change of basal CRH-1 activity [23]. Altogether, these results suggest that CRH-1 regulates distinct aspects of *C. elegans* development.

We have shown that an abundance of live OP50 food and high (2 μM) concentrations of ascr#5 (the most abundant ascaroside secreted when animals have grown at 20˚C) [7], which may reflect a natural condition of crowding at 20˚C but high food, do not induce dauer formation (L2d to dauer transition) but do induce L2d formation (L1 to L2d transition) in *crh-1* mutants. These results suggest CRH-1 is necessary to give the appropriate weight to pro-growth food cues in the environment such that the presence of pheromone in the environment is sufficient to promote L2d formation but not dauer commitment [4]. Moreover, ascr#5 but

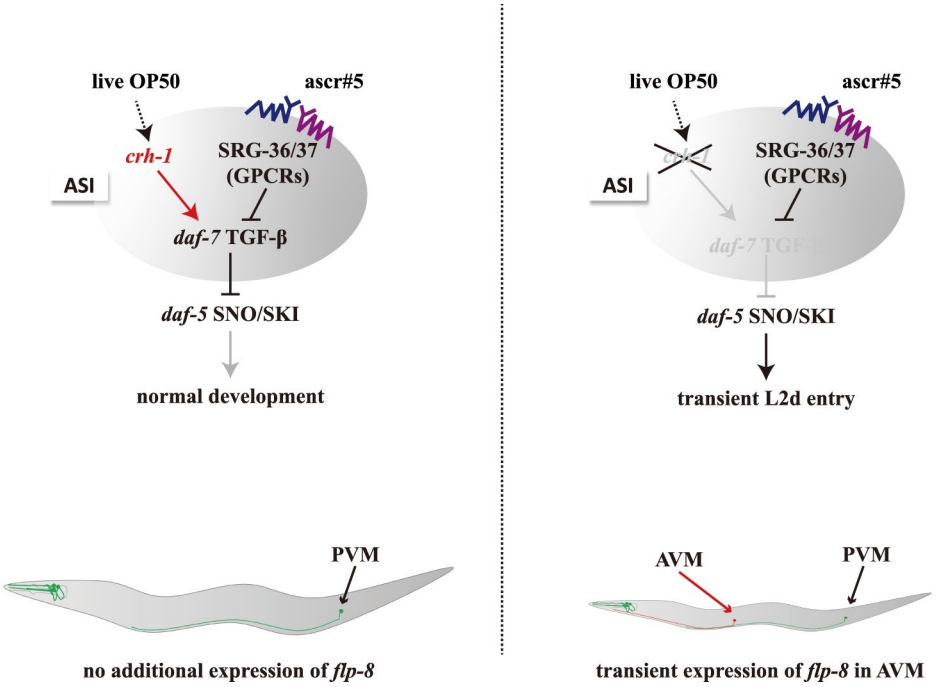

Fig 7. A model of the role of CRH-1 in ascr#5-mediated L2d formation. CRH-1 positively regulates dauer-inhibiting *daf-7* TGF-β expression in the ascr#5-sensing ASI neurons. In *crh-1* mutants, the decreased *daf-7* TGF-β expression provides a sensitized genetic background for further ascr#5-mediated *daf-7* TGF-β repression via *srg-36/37* GPCRs which leads to transient L2d formation and *flp-8* expression of AAP-TRN.

https://doi.org/10.1371/journal.pgen.1009678.g007

not ascr#2 or ascr#3 causes L2d formation in *crh-1* mutants, indicating that specific, but not all, pheromone component(s) may affect the decision for L1 to transition to L2 or L2d and worms weigh pheromone signals differently at different dauer decision points. ascr#5 is the most potent component of the dauer inducing ascaroside pheromones [7] and is produced in higher amounts in well-fed worms than in starved worms, indicating that ascr#5 may be a *bona fide* indicator of healthy populations or favorable environments [11]. Despite this hypothesis, very high (6 μM) concentrations of ascr#5 can elicit L2d formation in wild-type animals, indicating that *crh-1* mutants are precocious in L2d entry. Given that ascr#5 further reduces *daf-7* expression in the ASI neurons of *crh-1* mutants, we infer that CRH-1 acts as a food sensor to set the basal level of *daf-7* expression. Furthermore, the two-step process to enter dauer likely allows animals to be more flexible and adjust to rapidly changing environments [40].

Previously, a large number of genes have been shown to be differentially expressed in dauer larvae [41,42]. Interestingly, expression of most, but not all, *flp* genes, including *flp-8* are up-regulated during dauer development [42], and several *flp* genes have shown to be involved in dauer development and behaviors [42,43]. Since the *flp-8* expression in the AAP-TRN begins at the L2d stage and is maintained throughout the dauer stage, the function of FLP-8 neuropeptide in the AAP-TRN of L2d and dauer larvae is intriguing. Although the exact function of FLP-8 has not been determined, a family of FLP neuropeptides appears to inhibit overall circuit activity [44]. Previously, Chen and Chalfie [45] showed that dauer larvae exhibited reduced touch sensitivity. Thus, it is possible that FLP-8 expression in the AAP-TRN could inhibit circuit activity underlying touch sensation, which leads to decreased mechanosensation in dauer and likely L2d larvae. It would be the next question to be explored in the future.

Transforming growth factor β (TGF-β) signaling mediates diverse physiological roles, including cell differentiation, morphogenesis, tissue homeostasis, regeneration, and immune response, while the misregulation of TGF-β signaling promotes distinct disease states such as cancer progression (see review by Massague [46]). While cellular response pathways to secretion and diffusion/trafficking of the TGF-β ligand are well-characterized, relatively little is known about the regulation of its expression [47]. In *C. elegans*, TGF-β signaling regulates body size, innate immunity, aging, cell fate specification, differentiation, and dauer formation (see review by Savage and Padgett [48]). For example, TGF-β signaling regulates CREB activity in the hypodermis to mediate reproductive aging, and *crh-1* acts downstream of *sma-3* R-SMAD and regulates *wrt-10* Hedgehog-related signaling factor[49]. Although the downstream components of TGF-β signaling are evolutionarily conserved and well-characterized, upstream transcription factors and *cis*-regulatory elements by which expression of TGF-β genes is controlled are not as well characterized. Here, we have shown that the CREB homolog CRH-1 directly binds a novel CRE in the *daf-7* TGF-β promoter, which must integrate multiple external and internal signals and positively regulates its expression in the ASI neuroendocrine cells. Future studies are needed to identify potential CRH-1 co-factors, which may help to refine or modulate its actions at the *daf-7* promoter. Similar to mammalian CREB, *C. elegans* CRH-1 functions in many developmental and behavioral processes, including longevity, learning and memory, and now, developmental plasticity. Thus, CREB acts as a determinant of a context-dependent role of TGF-β signaling and provides a useful model to study TGF-β gene expression.

Materials and methods

Strains and constructs

The N2 Bristol strain was used as wild-type. All strains were maintained and grown on NGM agar plates seeded with *E. coli* OP50 at 20˚C [50]. All used strains in this study are listed in S1 Table. Promoters and cDNA used for rescue experiments of *crh-1* and *daf-7* were described in Park et al. [51]. The *daf-7* promoter (3127bp) for expression and CRE site analysis was produced by polymerase chain reactions using forward and reverse primers (see S2 Table) and subcloned into a pPD95.77 vector. The *nhr-246* promoter (3067bp) for expression was produced by polymerase chain reactions using forward primer 5'-aaaaaacctgcaggCACCGATGCGTTGTTATAGG-3' and reverse primer 5'-ttttttcccgggTGTTGAAATTGAAAATTATTTTGAA-3' [34] and subcloned into a pPD95.77 vector. All plasmids were injected at 0.1 ng (*flp-8* expression analysis), 10 ng (rescue experiments), or 50 ng (expression analysis) with *unc-122*p::*dsRed* as an injection marker.

Pheromone preparation and assay plates

Crude pheromone was prepared following the protocol described by Golden and Riddle (1984). Before assay, each crude pheromone batch was tested for its efficiency to induce dauer formation. The assay plates containing crude pheromone were prepared by spreading pheromone and drying for 3–4 h. The ascaroside pheromone components were chemically synthesized following Butcher et al. [6,7]. Before use, pheromone was diluted with dH_2O from a 3 mM stock solution of pheromone in 100% ethanol. For the assay plates containing synthetic ascarosides, the pheromone solution was mixed with agar solution before pouring.

L2d formation assay

Synchronized adult animals were placed onto 3.5 cm assay plates seeded with live OP50 and containing ethanol or pheromone at 25˚C and allowed to lay over 50 eggs for 1–2 h. Then,

adult animals were removed, and assay plates were placed at 25˚C for 40 h before observing the morphology of worms or marker gene expression and counting as L2d larvae. Dauer larvae and L2d larvae were selected based on the survival with 1% SDS treatment [5].

Dauer formation assay

A dauer formation assay was performed as previously described by Golden and Riddle [4] and Neal et al. [52]. Synchronized adult animals were allowed to lay eggs at 25˚C for 4–5 h on 3.5 cm assay plates. After the plates contained approximately 65–85 eggs/plate, adult animals were removed, and the plates were placed at 25˚C for 68–72 h. Dauer and non-dauer animals were identified by visual inspection. Assay plates were made with Noble agar (BD Biosciences) lacking peptone. Heat-killed OP50 bacteria were seeded on each plate. For each experiment, all strains were assayed in parallel in at least four independent experiments.

daf-7 smFISH

daf-7 smFISH was performed as previously described by Meisel et al. [16] by using the Stellaris smFISH fluorescent probe and buffer sets (Biosearch). Worms were washed in 1XPBS and fixed in 3.7% formaldehyde in PBS for 45 min at 4˚C and rinsed twice with 1XPBS. Then, worms were immersed in 70% ethanol for 24 h at 4˚C and washed by buffer A (Biosearch) for 5 minutes at room temperature. Then, a hybridization buffer containing the *daf-7* probe (125 nM, Biosearch) was added and incubated overnight at 30˚C. Worms were washed twice with buffer A. Then, worms were mounted onto glass slides by mounting medium (Sigma). All smFISH images were acquired by a Zeiss Axio Imager using 63x objectives and a CCD camera (Hamamatsu). Quantification was performed using ImageJ software to extract mean intensity and regions of interest. The relative mean intensity of fluorescence was normalized by area.

Quantification of GFP expression

For GFP quantification, the worms were anesthetized in sodium azide on an agar pad, and GFP fluorescence was observed with a Zeiss Axio Imager using 40x (for the adult stage) and 63x (for L1) objectives and a CCD camera (Hamamatsu). The relative expression level of GFP was measured at each developmental stage. The relative GFP levels were rated from 1 (dim) to 5 (bright) by visual inspection, and these values were confirmed using Image J software.

SEM (Scanning Electron Microscope) imaging

Samples were prepared by critical point dryer (Leica EM CPD300) after sequential ethanol dehydration. Dried samples were coated with gold using a sputter coater and then were imaged with a HR FE-SEM (Hitachi, SU8020, CCRF DGIST).

Electrophoretic mobility shift assay (EMSA)

Nuclear extract preparation from HEK293T cells and in vitro EMSA reactions were carried out as previously described Kim et al. [53], and biotinylated EMSA probes and unlabeled competitor probes were synthesized by using a LightShift Chemiluminescent EMSA Kit (Thermo Scientific). The *daf-7*p-WT-CRE and *daf-7*p-mut-CRE probes with the following sequences were employed:

*daf-7*p-WT-CRE: 5' attagggtacgtacgtcaatattagggtacgtacgtcaatattagggtacgtacgtcaat 3' (60 mer)

*daf-7*p- mut-CRE: 5' attagggtatttttttcaatattagggtatttttttcaatattagggtatttttttcaat 3' (60 mer)

Statistical anlaysis

Statistical anlaysis were performed using GraphPad Prism 8.0 and Microsoft Excel 365. Data used for statistical analysis are in the S1 Data file.

Supporting information

S1 Fig. *crh-1* mutants form transient predauer (L2d) larvae. Shown are the survival rate of wild-type, *crh-1* mutant and *daf-7* mutants animals under 1% sodium dodecyl sulfate (SDS) treatment. Two independent assays with n>50.
(PDF)

S2 Fig. *daf-7* mutants exhibit strong expression of *flp-8* in the AVM in non dauer-inducing conditions. Shown are images of *flp-8*p::*gfp* expression in the AVM in *daf-7* mutants at 45 and 60 hAH. The boxed regions of the first column are shown on the right columns at higher magnification. hAH, hour after hatching. Scale bars: 50 μm.
(PDF)

S3 Fig. *crh-1* mutants exhibit expression of *flp-8* in the AAP-TRN in dauer-inducing conditions. Percent of *flp-8*p::*gfp* expression in the AVM, ALM and PLM neurons by wild-type or *crh-1* mutant animals when grown in the presence of heat-killed OP50 food and ascr#5 pheromone. $n \geq 30$ for each. hAH, hour after hatching. Error bars indicate SEM. * and ** indicate different from wild-type at $p < 0.05$ and $p < 0.01$, respectively (student t-test).
(PDF)

S4 Fig. ascr#5 is required for *flp-8*p::*gfp* expression in the AAP-TRN in wild-type or *crh-1* mutant animals. Percent of *flp-8*p::*gfp* expression in the AVM, ALM and PLM neurons by wild-type or *crh-1* mutant animals when grown in the presence of heat-killed OP50 food (left) or live OP50 (right). $n \geq 30$ for each. hAH, hour after hatching. Error bars indicate SEM. * indicates different from wild-type at $p < 0.05$ (student t-test).
(PDF)

S5 Fig. *crh-1* mutants exhibit expression of *nhr-246* in the intestine in non dauer-inducing conditions. Shown are left images of *nhr-246*p::*gfp* expression in the intestine of *crh-1* mutants at 45, 50, and 55 hAH. The boxed regions of the second column are shown on the right columns at higher magnification. Scale bars: 50 μm. Shown is the right panel of the percent of *nhr-246*p::*gfp* expression in the intestine by wild-type or *crh-1* mutant animals when grown in the presence of live OP50 food and ascr#5 pheromone at 45, 50, and 55 hAH. hAH, hour after hatching. $n \geq 20$ for each. Error bars indicate SEM. *** indicates different from wild-type at $p < 0.001$ (student t-test).
(PDF)

S6 Fig. *crh-1* mutants exhibit normal or weakly decreased pheromone-mediated dauer formation. Percent of dauer formed by wild-type or *crh-1* mutant animals when grown in the presence of heat-killed OP50 food and ascr#5, ascr#2, or ascr#3 pheromone.
(PDF)

S7 Fig. *crh-1* mutants form L2d larvae in a non-dauer inducing condition. Percent of L2d formed by wild-type or *crh-1* mutant animals when grown in the presence of live OP50 food and crude pheromone. $N \geq 5$ for each. Error bars indicate SEM. *, **, and *** indicate different from wild-type at $p < 0.05$, $p < 0.01$, and $p < 0.001$, respectively (student t-test).
(PDF)

S8 Fig. Morphology of mouths of wild-type L3 larva, *crh-1* mutant L2d larva, and wild-type dauer larva. Shown are images of scanning electron microscopy. Scale bar: 5μm (top) and 100μm (bottom).
(PDF)

S9 Fig. *crh-1* mutants do not form L2d larvae in the presence of ascr#2. Percent of L2d formed by wild-type or *crh-1* mutant animals when grown in the presence of live OP50 food and three different concentrations of ascr#2 pheromone. N ≥ 5 for each.
(PDF)

S10 Fig. *crh-1* mutants do not exhibit *flp-8* expression in the AAP-TRN in response to ascr#2 and ascr#3. Percent of *flp-8*p::*gfp* expression in the AVM, ALM and PLM neurons by wild-type or *crh-1* mutant animals when grown in the presence of live OP50 and ascr#2 or ascr#3. n ≥ 30 for each. hAH, hour after hatching. Error bars indicate SEM.
(PDF)

S11 Fig. The ASI morphology and dye-filling properties are not altered in the *crh-1* mutants. Shown are images of wild-type or *crh-1* mutant animals expressing *gpa-4*p::*gfp* transgene or stained with DiI. Scale bar: 10 μm.
(PDF)

S12 Fig. *daf-16* mutation does not affect the L2d formation of *crh-1* mutants. Percent of L2d formed by animals of the indicated genotypes when grown in the presence of live OP50 food and ascr#5 pheromone. N ≥ 4 for each. Error bars indicate SEM. N.S. not significantly different (one-way ANOVA with Bonferroni's post hoc tests).
(PDF)

S13 Fig. Mutation in CRE motif of *daf-7* promoter does not affect *daf-7* expression in the ASJ neurons. The percentage of transgenic animals expressing *daf-7*p::*gfp* reporter construct in the ASJ neurons is shown. GFP fluorescence was observed either in wild-type or *crh-1* mutant animals. The Strength of GFP expression is indicated by the number of + symbols. Wild-type nucleotides are indicated in red, mutated nucleotides in blue. An arrowhead indicates *daf-7*p-mutated CRE promoter. At least two independent extrachromosomal lines for each construct were examined. n ≥ 30 for each.
(PDF)

S1 Table. List of strains used in this work.
(DOCX)

S2 Table. List of primers and probes used in *daf-7* related work.
(DOCX)

S1 Data. Excel of raw data file of all relevant figures.
(XLSX)

Acknowledgments

We would like to thank the *Caenorhabditis* Genetics Center (NIH Office of Research Infrastructure Programs, P40 OD010440), the National BioResource Project (Japan) and Chris Li for strains. We also would like to thank Dennis H. Kim, Seung-Jae V. Lee, Sun-Kyung Lee, and K. Kim lab members for their helpful comments and discussion on the manuscript.

Author Contributions

Conceptualization: JiSoo Park, Scott J. Neal, Piali Sengupta, Dae-Won Kim, Kyuhyung Kim.

Data curation: JiSoo Park, Hyekyoung Oh, Do-Young Kim, YongJin Cheon, Yeon-Ji Park, Hyeonjeong Hwang.

Formal analysis: JiSoo Park, Hyekyoung Oh, Do-Young Kim, YongJin Cheon, Yeon-Ji Park, Hyeonjeong Hwang.

Investigation: Scott J. Neal, Piali Sengupta, Dae-Won Kim, Kyuhyung Kim.

Methodology: Hyekyoung Oh, Do-Young Kim, YongJin Cheon, Yeon-Ji Park, Hyeonjeong Hwang.

Resources: Abdul Rouf Dar, Rebecca A. Butcher.

Supervision: Dae-Won Kim, Kyuhyung Kim.

Validation: Kyuhyung Kim.

Writing – original draft: JiSoo Park, Kyuhyung Kim.

Writing – review & editing: JiSoo Park, Do-Young Kim, YongJin Cheon, Yeon-Ji Park, Hyeonjeong Hwang, Scott J. Neal, Piali Sengupta, Dae-Won Kim, Kyuhyung Kim.

References

1. Vellichirammal NN, Gupta P, Hall TA, Brisson JA. Ecdysone signaling underlies the pea aphid transgenerational wing polyphenism. Proc Natl Acad Sci U S A. 2017; 114(6):1419–23. https://doi.org/10.1073/pnas.1617640114 PMID: 28115695; PubMed Central PMCID: PMC5307454.
2. Projecto-Garcia J, Biddle JF, Ragsdale EJ. Decoding the architecture and origins of mechanisms for developmental polyphenism. Curr Opin Genet Dev. 2017; 47:1–8. https://doi.org/10.1016/j.gde.2017.07.015 PMID: 28810163.
3. Fusco G, Minelli A. Phenotypic plasticity in development and evolution: facts and concepts. Introduction. Philos Trans R Soc Lond B Biol Sci. 2010; 365(1540):547–56. Epub 2010/01/20. https://doi.org/10.1098/rstb.2009.0267 PMID: 20083631; PubMed Central PMCID: PMC2817147.
4. Golden JW, Riddle DL. The Caenorhabditis elegans dauer larva: developmental effects of pheromone, food, and temperature. Dev Biol. 1984; 102(2):368–78. Epub 1984/04/01. https://doi.org/10.1016/0012-1606(84)90201-x PMID: 6706004.
5. Cassada RC, Russell RL. The dauerlarva, a post-embryonic developmental variant of the nematode Caenorhabditis elegans. Dev Biol. 1975; 46(2):326–42. Epub 1975/10/01. https://doi.org/10.1016/0012-1606(75)90109-8 PMID: 1183723.
6. Butcher RA, Fujita M, Schroeder FC, Clardy J. Small-molecule pheromones that control dauer development in Caenorhabditis elegans. Nat Chem Biol. 2007; 3(7):420–2. Epub 2007/06/15. https://doi.org/10.1038/nchembio.2007.3 PMID: 17558398.
7. Butcher RA, Ragains JR, Kim E, Clardy J. A potent dauer pheromone component in Caenorhabditis elegans that acts synergistically with other components. Proc Natl Acad Sci U S A. 2008; 105(38):14288–92. https://doi.org/10.1073/pnas.0806676105 PMID: 18791072; PubMed Central PMCID: PMC2567175.
8. Jeong PY, Jung M, Yim YH, Kim H, Park M, Hong E, et al. Chemical structure and biological activity of the Caenorhabditis elegans dauer-inducing pheromone. Nature. 2005; 433(7025):541–5. Epub 2005/02/04. https://doi.org/10.1038/nature03201 PMID: 15690045.
9. Srinivasan J, Kaplan F, Ajredini R, Zachariah C, Alborn HT, Teal PE, et al. A blend of small molecules regulates both mating and development in Caenorhabditis elegans. Nature. 2008; 454(7208):1115–8. Epub 2008/07/25. https://doi.org/10.1038/nature07168 PMID: 18650807; PubMed Central PMCID: PMC2774729.
10. Kaplan F, Srinivasan J, Mahanti P, Ajredini R, Durak O, Nimalendran R, et al. Ascaroside expression in Caenorhabditis elegans is strongly dependent on diet and developmental stage. PLoS One. 2011; 6(3):e17804. https://doi.org/10.1371/journal.pone.0017804 PMID: 21423575; PubMed Central PMCID: PMC3058051.

11. von Reuss SH, Bose N, Srinivasan J, Yim JJ, Judkins JC, Sternberg PW, et al. Comparative metabolomics reveals biogenesis of ascarosides, a modular library of small-molecule signals in C. elegans. J Am Chem Soc. 2012; 134(3):1817–24. https://doi.org/10.1021/ja210202y PMID: 22239548; PubMed Central PMCID: PMC3269134.

12. Ren P, Lim CS, Johnsen R, Albert PS, Pilgrim D, Riddle DL. Control of C. elegans larval development by neuronal expression of a TGF-beta homolog. Science. 1996; 274(5291):1389–91. Epub 1996/11/22. https://doi.org/10.1126/science.274.5291.1389 PMID: 8910282.

13. Schackwitz WS, Inoue T, Thomas JH. Chemosensory neurons function in parallel to mediate a pheromone response in C. elegans. Neuron. 1996; 17(4):719–28. Epub 1996/10/01. https://doi.org/10.1016/s0896-6273(00)80203-2 PMID: 8893028.

14. Kimura KD, Tissenbaum HA, Liu Y, Ruvkun G. daf-2, an insulin receptor-like gene that regulates longevity and diapause in Caenorhabditis elegans. Science. 1997; 277(5328):942–6. Epub 1997/08/15. https://doi.org/10.1126/science.277.5328.942 PMID: 9252323.

15. Kim K, Sato K, Shibuya M, Zeiger DM, Butcher RA, Ragains JR, et al. Two chemoreceptors mediate developmental effects of dauer pheromone in C. elegans. Science. 2009; 326(5955):994–8. Epub 2009/10/03. https://doi.org/10.1126/science.1176331 PMID: 19797623; PubMed Central PMCID: PMC4448937.

16. Meisel JD, Panda O, Mahanti P, Schroeder FC, Kim DH. Chemosensation of bacterial secondary metabolites modulates neuroendocrine signaling and behavior of C. elegans. Cell. 2014; 159(2):267–80. Epub 2014/10/11. https://doi.org/10.1016/j.cell.2014.09.011 PMID: 25303524; PubMed Central PMCID: PMC4194030.

17. Kimura Y, Corcoran EE, Eto K, Gengyo-Ando K, Muramatsu MA, Kobayashi R, et al. A CaMK cascade activates CRE-mediated transcription in neurons of Caenorhabditis elegans. EMBO Rep. 2002; 3 (10):962–6. Epub 2002/09/17. https://doi.org/10.1093/embo-reports/kvf191 PMID: 12231504; PubMed Central PMCID: PMC1307624.

18. Suo S, Kimura Y, Van Tol HH. Starvation induces cAMP response element-binding protein-dependent gene expression through octopamine-Gq signaling in Caenorhabditis elegans. J Neurosci. 2006; 26 (40):10082–90. https://doi.org/10.1523/JNEUROSCI.0819-06.2006 PMID: 17021164; PubMed Central PMCID: PMC6674634.

19. Kauffman AL, Ashraf JM, Corces-Zimmerman MR, Landis JN, Murphy CT. Insulin signaling and dietary restriction differentially influence the decline of learning and memory with age. PLoS Biol. 2010; 8(5): e1000372. https://doi.org/10.1371/journal.pbio.1000372 PMID: 20502519; PubMed Central PMCID: PMC2872642.

20. Nishida Y, Sugi T, Nonomura M, Mori I. Identification of the AFD neuron as the site of action of the CREB protein in Caenorhabditis elegans thermotaxis. EMBO Rep. 2011; 12(8):855–62. https://doi.org/10.1038/embor.2011.120 PMID: 21738224; PubMed Central PMCID: PMC3147260.

21. Timbers TA, Rankin CH. Tap withdrawal circuit interneurons require CREB for long-term habituation in Caenorhabditis elegans. Behav Neurosci. 2011; 125(4):560–6. https://doi.org/10.1037/a0024370 PMID: 21688885.

22. Yu YV, Bell HW, Glauser D, Van Hooser SD, Goodman MB, Sengupta P. CaMKI-dependent regulation of sensory gene expression mediates experience-dependent plasticity in the operating range of a thermosensory neuron. Neuron. 2014; 84(5):919–26. https://doi.org/10.1016/j.neuron.2014.10.046 PMID: 25467978; PubMed Central PMCID: PMC4258139.

23. Lakhina V, Arey RN, Kaletsky R, Kauffman A, Stein G, Keyes W, et al. Genome-wide functional analysis of CREB/long-term memory-dependent transcription reveals distinct basal and memory gene expression programs. Neuron. 2015; 85(2):330–45. Epub 2015/01/23. https://doi.org/10.1016/j.neuron.2014.12.029 PMID: 25611510; PubMed Central PMCID: PMC4340687.

24. Chen YC, Chen HJ, Tseng WC, Hsu JM, Huang TT, Chen CH, et al. A C. elegans Thermosensory Circuit Regulates Longevity through crh-1/CREB-Dependent flp-6 Neuropeptide Signaling. Dev Cell. 2016; 39(2):209–23. https://doi.org/10.1016/j.devcel.2016.08.021 PMID: 27720609.

25. Moss BJ, Park L, Dahlberg CL, Juo P. The CaM Kinase CMK-1 Mediates a Negative Feedback Mechanism Coupling the C. elegans Glutamate Receptor GLR-1 with Its Own Transcription. PLoS Genet. 2016; 12(7):e1006180. https://doi.org/10.1371/journal.pgen.1006180 PMID: 27462879; PubMed Central PMCID: PMC4963118.

26. Freytag V, Probst S, Hadziselimovic N, Boglari C, Hauser Y, Peter F, et al. Genome-Wide Temporal Expression Profiling in Caenorhabditis elegans Identifies a Core Gene Set Related to Long-Term Memory. J Neurosci. 2017; 37(28):6661–72. https://doi.org/10.1523/JNEUROSCI.3298-16.2017 PMID: 28592692; PubMed Central PMCID: PMC6596549.

27. Nishijima S, Maruyama IN. Appetitive Olfactory Learning and Long-Term Associative Memory in Caenorhabditis elegans. Front Behav Neurosci. 2017; 11:80. https://doi.org/10.3389/fnbeh.2017.00080 PMID: 28507513; PubMed Central PMCID: PMC5410607.

28. Arey RN, Stein GM, Kaletsky R, Kauffman A, Murphy CT. Activation of Galphaq Signaling Enhances Memory Consolidation and Slows Cognitive Decline. Neuron. 2018; 98(3):562–74 e5. https://doi.org/10.1016/j.neuron.2018.03.039 PMID: 29656871; PubMed Central PMCID: PMC5934306.

29. Kaletsky R, Yao V, Williams A, Runnels AM, Tadych A, Zhou S, et al. Transcriptome analysis of adult Caenorhabditis elegans cells reveals tissue-specific gene and isoform expression. PLoS Genet. 2018; 14(8):e1007559. https://doi.org/10.1371/journal.pgen.1007559 PMID: 30096138; PubMed Central PMCID: PMC6105014.

30. Altarejos JY, Montminy M. CREB and the CRTC co-activators: sensors for hormonal and metabolic signals. Nat Rev Mol Cell Biol. 2011; 12(3):141–51. https://doi.org/10.1038/nrm3072 PMID: 21346730; PubMed Central PMCID: PMC4324555.

31. Kim K, Li C. Expression and regulation of an FMRFamide-related neuropeptide gene family in Caenorhabditis elegans. J Comp Neurol. 2004; 475(4):540–50. https://doi.org/10.1002/cne.20189 PMID: 15236235.

32. Butcher RA. Small-molecule pheromones and hormones controlling nematode development. Nat Chem Biol. 2017; 13(6):577–86. https://doi.org/10.1038/nchembio.2356 PMID: 28514418; PubMed Central PMCID: PMC5809121.

33. Croll NA, Smith JM, Zuckerman BM. The aging process of the nematode Caenorhabditis elegans in bacterial and axenic culture. Exp Aging Res. 1977; 3(3):175–89. https://doi.org/10.1080/03610737708257101 PMID: 334555.

34. Shih PY, Lee JS, Sternberg PW. Genetic markers enable the verification and manipulation of the dauer entry decision. Dev Biol. 2019; 454(2):170–80. https://doi.org/10.1016/j.ydbio.2019.06.009 PMID: 31242447.

35. McGrath PT, Xu Y, Ailion M, Garrison JL, Butcher RA, Bargmann CI. Parallel evolution of domesticated Caenorhabditis species targets pheromone receptor genes. Nature. 2011; 477(7364):321–5. Epub 2011/08/19. https://doi.org/10.1038/nature10378 PMID: 21849976; PubMed Central PMCID: PMC3257054.

36. Nolan KM, Sarafi-Reinach TR, Horne JG, Saffer AM, Sengupta P. The DAF-7 TGF-beta signaling pathway regulates chemosensory receptor gene expression in C. elegans. Genes Dev. 2002; 16(23):3061–73. Epub 2002/12/05. https://doi.org/10.1101/gad.1027702 PMID: 12464635; PubMed Central PMCID: PMC187495.

37. Patterson GI, Koweek A, Wong A, Liu Y, Ruvkun G. The DAF-3 Smad protein antagonizes TGF-beta-related receptor signaling in the Caenorhabditis elegans dauer pathway. Genes Dev. 1997; 11(20):2679–90. Epub 1997/10/23. https://doi.org/10.1101/gad.11.20.2679 PMID: 9334330; PubMed Central PMCID: PMC316611.

38. da Graca LS, Zimmerman KK, Mitchell MC, Kozhan-Gorodetska M, Sekiewicz K, Morales Y, et al. DAF-5 is a Ski oncoprotein homolog that functions in a neuronal TGF beta pathway to regulate C. elegans dauer development. Development. 2004; 131(2):435–46. Epub 2003/12/19. https://doi.org/10.1242/dev.00922 PMID: 14681186.

39. Comb M, Birnberg NC, Seasholtz A, Herbert E, Goodman HM. A cyclic AMP- and phorbol ester-inducible DNA element. Nature. 1986; 323(6086):353–6. https://doi.org/10.1038/323353a0 PMID: 3020428.

40. Avery L. A model of the effect of uncertainty on the C elegans L2/L2d decision. PLoS One. 2014; 9(7):e100580. Epub 2014/07/17. https://doi.org/10.1371/journal.pone.0100580 PMID: 25029446; PubMed Central PMCID: PMC4100763.

41. Wang J, Kim SK. Global analysis of dauer gene expression in Caenorhabditis elegans. Development. 2003; 130(8):1621–34. https://doi.org/10.1242/dev.00363 PMID: 12620986.

42. Lee JS, Shih PY, Schaedel ON, Quintero-Cadena P, Rogers AK, Sternberg PW. FMRFamide-like peptides expand the behavioral repertoire of a densely connected nervous system. Proc Natl Acad Sci U S A. 2017; 114(50):E10726–E35. https://doi.org/10.1073/pnas.1710374114 PMID: 29167374; PubMed Central PMCID: PMC5740649.

43. Cohen M, Reale V, Olofsson B, Knights A, Evans P, de Bono M. Coordinated regulation of foraging and metabolism in C. elegans by RFamide neuropeptide signaling. Cell Metab. 2009; 9(4):375–85. https://doi.org/10.1016/j.cmet.2009.02.003 PMID: 19356718.

44. Li C, Kim K. Family of FLP Peptides in Caenorhabditis elegans and Related Nematodes. Front Endocrinol (Lausanne). 2014; 5:150. https://doi.org/10.3389/fendo.2014.00150 PMID: 25352828; PubMed Central PMCID: PMC4196577.

45. Chen X, Chalfie M. Modulation of C. elegans touch sensitivity is integrated at multiple levels. J Neurosci. 2014; 34(19):6522–36. https://doi.org/10.1523/JNEUROSCI.0022-14.2014 PMID: 24806678; PubMed Central PMCID: PMC4012311.

46. Massague J. TGFbeta in Cancer. Cell. 2008; 134(2):215–30. https://doi.org/10.1016/j.cell.2008.07.001 PMID: 18662538; PubMed Central PMCID: PMC3512574.

47. Kim SJ, Jeang KT, Glick AB, Sporn MB, Roberts AB. Promoter sequences of the human transforming growth factor-beta 1 gene responsive to transforming growth factor-beta 1 autoinduction. J Biol Chem. 1989; 264(12):7041–5. PMID: 2708352.

48. Savage-Dunn C, Padgett RW. The TGF-beta Family in Caenorhabditis elegans. Cold Spring Harb Perspect Biol. 2017; 9(6). https://doi.org/10.1101/cshperspect.a022178 PMID: 28096268; PubMed Central PMCID: PMC5453393.

49. Templeman NM, Cota V, Keyes W, Kaletsky R, Murphy CT. CREB Non-autonomously Controls Reproductive Aging through Hedgehog/Patched Signaling. Dev Cell. 2020; 54(1):92–105 e5. https://doi.org/10.1016/j.devcel.2020.05.023 PMID: 32544391; PubMed Central PMCID: PMC7837322.

50. Brenner S. The genetics of Caenorhabditis elegans. Genetics. 1974; 77(1):71–94. PMID: 4366476; PubMed Central PMCID: PMC1213120.

51. Park J, Choi W, Dar AR, Butcher RA, Kim K. Neuropeptide Signaling Regulates Pheromone-Mediated Gene Expression of a Chemoreceptor Gene in C. elegans. Mol Cells. 2019; 42(1):28–35. https://doi.org/10.14348/molcells.2018.0380 PMID: 30453729; PubMed Central PMCID: PMC6354054.

52. Neal SJ, Kim K, Sengupta P. Quantitative assessment of pheromone-induced Dauer formation in Caenorhabditis elegans. Methods Mol Biol. 2013; 1068:273–83. Epub 2013/09/10. https://doi.org/10.1007/978-1-62703-619-1_20 PMID: 24014369.

53. Kim DW, Kempf H, Chen RE, Lassar AB. Characterization of Nkx3.2 DNA binding specificity and its requirement for somitic chondrogenesis. J Biol Chem. 2003; 278(30):27532–9. https://doi.org/10.1074/jbc.M301461200 PMID: 12746429.